SMAR 2015 – Third Conference on Smart Monitoring,
Assessment and Rehabilitation of Civil Structures

SMAR 2015

Behavior of mullions formed in non-structural RC partition walls with openings

Yo Hibino[1], Dong Zha[2], and Ryosuke Takahashi[3]

[1] Hiroshima University, Higashihiroshima, Japan
[2] Hiroshima University, Higashihiroshima, Japan
[3] Haseko Corporation, Osaka, Japan

ABSTRACT: Mullions formed in-plane with non-structural reinforced concrete (RC) partition walls with openings, found in residential buildings, were severely damaged in 1995 Kobe and 2011 Tohoku earthquakes without any noticeable damage on their boundary beams and columns. Damage of such non-structural elements does not affect design strength of buildings but leads to damage of surroundings fittings. Hence, investigation of behavior of the non-structural RC partition walls is necessary for damage mitigation. In this study, experimental tests with a series of specimens simulates mullions formed in non-structural RC partition walls with openings in one-bay frame designed on the basis of weak beam and strong column concept were conducted. From the experimental result, deformation behavior of mullions formed in non-structural RC partition walls involved with deformation of boundaries was evaluated and their failure mechanisms were investigated.

1 INTRODUCTIONS

Mullions formed in-plane with non-structural reinforced concrete (RC) partition walls with openings are found in residential buildings, which were severely damaged in 1995 Kobe and 2011 Tohoku earthquakes without any noticeable damage on their boundary beams and columns as shown in Figure 1. Damage of non-structural member is accepted in structural design in Japan not to bring damage of structural members; however, the damage leads to damage of surrounding fittings which disturb daily business. Recently, although non-structural reinforced concrete walls are fabricated with slit (Okubo, 2009) to avoid damage, it is preferable to construct non-structural walls without slit in consideration of cost of construction and strength. Especially, mullions is susceptible to be damaged due to their low bearing capacity, hence, to evaluate behavior of mullions is necessary to preserve function of buildings and to prevent damage of non-structural walls. Additionally, in recent buildings flexural deformation of boundary beams is predominant without shear failure of columns because beams are designed to yield prior to columns to establish a design concept of weak beam and strong columns, which may enhance damage of non-structural walls joined with beams. Therefore, in this study experimental test of a series of specimen simulates one-bay frame with mullions formed in non-structural wall were conducted, and investigated behavior of mullions and failure mechanism considering axial force on mullion involved with beam deformation.

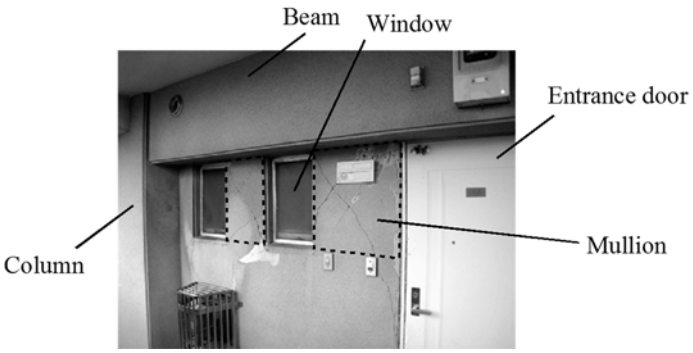

Figure 1. Damage of mullions formed in non-structural RC partition walls in 2011 Tohoku earthquakes.

2 EXPERIMENTAL INVESTIGATION

2.1 Test specimens

There are three specimens assuming one-bay frame with non-structural RC partition walls with openings which properties are shown in Table 1. They were fabricated as 1/4 scale frames assuming in mid-story RC condominium buildings in Japan and the geometric properties are shown in Figure 2. Two mullions are formed next to openings represent windows and entrance of residence. The geometry and reinforcement of mullions are different between specimens: vertical and horizontal reinforcement of 0.35% used for the specimen B-WOA; horizontal reinforcement of 0.35% and vertical reinforcement of 0.7% used for the specimen BH-WOA-V; and vertical and horizontal reinforcement of 1.6% used for the specimen BH-WOA-VH. The longitudinal reinforcement in beams and columns are arranged to control order of their yielding. Normal strength of deformed steel bars are used in beams for all the specimens whereas above 390 MPa and 785 MPa strength deformed steel bars are used in columns in order that column reinforcements yield prior to beam reinforcements. The compressive strengths of concrete were targeted as 21 MPa for all specimens. The material properties of concrete and steel are shown in Table 2 and Table 3, respectively.

Table 1. Test specimen details

Member	Property	B-WOA	BH-WOA-V	BH-WOA-VH
Column	Cross Section, mm	220×220	220×220	220×220
	Longitudinal steel (ρ_l)	8-D13 (2.10)	8-K13 (2.10)	8-K13 (2.10)
	Transverse stirrup steel (ρ_t)	D6@50 (0.58)	RB7.1@50 (0.73)	RB7.1@50 (0.73)
Beam	Cross Section, mm	180×240	180×240	180×240
	Longitudinal steel (ρ_l)	8-D13 (2.35)	8-D13 (2.35)	8-D13 (2.35)
	Transverse stirrup steel (ρ_t)	D6@100 (0.71)	D6@100 (0.71)	D6@100 (0.71)
Wall	Cross Section, mm	40×1300	40×1300	40×1300
	Cross section of mullion, mm	180×250	170×250	170×250
	Vertical reinforcement (ρ_{vt})	D4@100 (0.35)	D4@50 (0.7)	D6@50 (1.6)
	Horizontal reinforcement (ρ_{ht})	D4@100 (0.35)	D4@100 (0.35)	D6@50 (1.6)

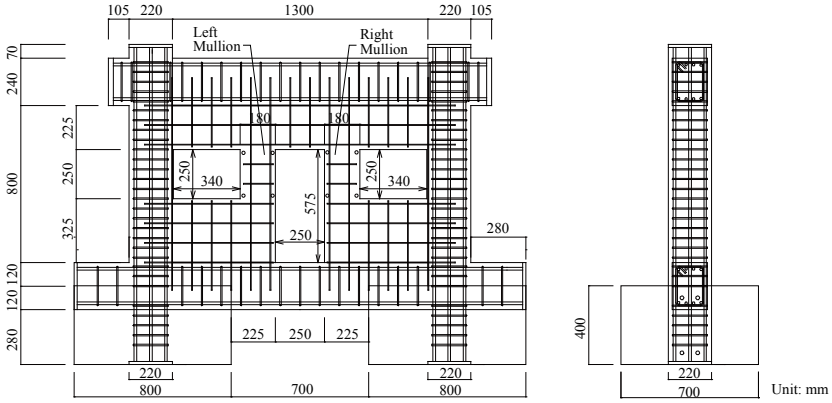

Figure 2. Configuration of test specimen (B-WOA)

Table 2. Concrete properties

	B-WOA	BH-WOA-V	BH-WOA-VH
Compressive strength, f_c' (MPa)	20.7	23.1	25.2
Splitting tensile strength, f_{ct}' (MPa)	23.1	2.40	2.36
Elastic moduls, E_c (GPa)	25.2	2.36	23.3

Table 3. Steel properties

No.	Strength	Specimen	Yield strength f_c' (MPa)	Tensile strength f_{ct}' (MPa)	Elastic modulus, E_c (GPa)
D4	SD295A	B-WOA	312	454	157
D4	SD295A	BH-WOA-V, BH-WOA-VH	356	528	193
D6	SD295A	B-WOA	350	530	194
D6	SD295A	BH-WOA-V, BH-WOA-VH	410	555	208
RB7.1	SBPD1275	BH-WOA-V, BH-WOA-VH	1481	1499	218
D13	SD345	B-WOA	382	541	180
D13	SD345	BH-WOA-V, BH-WOA-VH	408	578	203
D13	SD390	B-WOA	475	622	185
K13	KW785	BH-WOA-V, BH-WOA-VH	930	1090	208

2.2 Test setup

Bi-directional single-curvature lateral cyclic loading tests were conducted using the test rig shown in Figure 3. Axial loads assigned by vertical jack through a rigid girder installed above specimen are applied to each column with pin and roller supports. A constant axial load, simulating gravity load which magnitude was equal to 20% of the gross area of column section times concrete compressive strength, was applied during testing. The cyclic lateral load was applied by horizontal jack installed on upper beam at only odd side. The plus and minus beside arrow symbol shown in Figure 3 represent loading direction of loadings. A pin support with reaction block at the end of opposite to horizontal jack is connected with four high tension steel bars in order to transmit

compression force to the specimen from the end of opposite to horizontal jack on loadings in negative direction. The lateral cyclic loading was applied to each specimen to drift revels of ±0.125%×1, ±0.25%×2, ±0.5%×2, ±1%×2, ±1.5%×2, and ±2%×1. The drift level is the relative displacement between the center of a beam height and base of a column divided by its height (1040 mm).

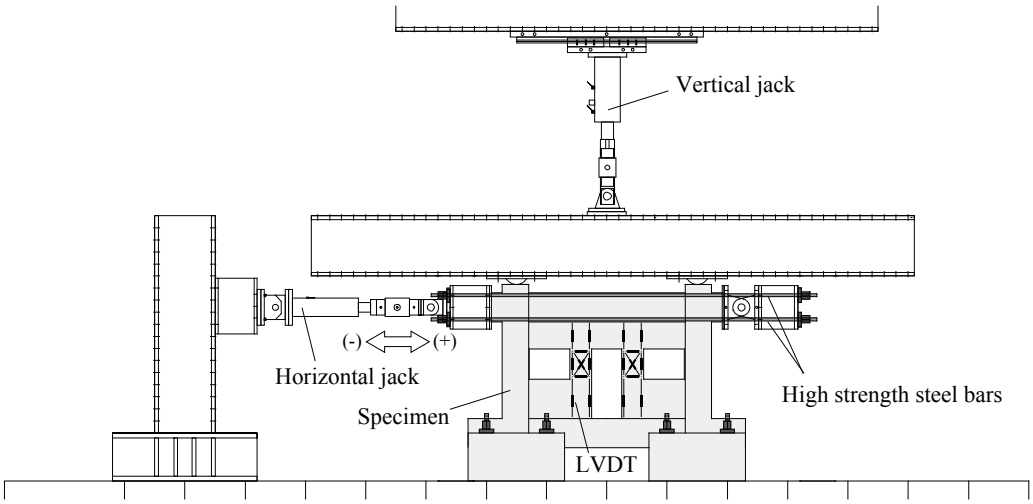

Figure 3. Test setup

3 EXPERIMENTAL RESULTS AND DISCUSSION

3.1 Load-deflection response and cracks

Figure 4 plots the lateral load-drift response of the specimens with maximum point indicated in the plots. The vertical axis represents the lateral load and horizontal axis represents the lateral drift. The maximum load, shown by open circle symbol, was observed at 1% drift for all specimens. Specimen BH-WOA-VH achieved a maximum load of 336kN which is approximately 120% of the maximum load of specimen B-WOA, which are summarized in Table 4 with average shear stress at ultimate strength τ_u and normalized shear stress τ_u/f'_c. All specimens had shear failure of mullions and bond splitting failure of columns at a degraded strength. At 1.5% drift, yielding of longitudinal reinforcement of column was observed for specimen B-WOA due to normal strength of reinforcements, whereas no yielding of longitudinal reinforcement of both beams and columns were observed for specimens BH-WOA-V and BH-WOA-VH. The normalized shear stresses τ_u/f'_c. for all specimens are equal to 0.12, which are smaller than typical normalized stress of reinforced concrete shear walls, in spite of difference of the amount of reinforcement and concrete compressive stress.

The crack patterns at the first full cycle to drift of 1% are shown in Figure 5. During testing, flexural cracks appeared on both mullions at first full cycle to 0.125 % drift, and diagonal shear cracks appeared on the right mullion only for specimens B-WOA and BH-WOA-VH. As the drift was increased further, shear cracks appeared on left mullion and extending to breast wall. Flexural cracks and shear cracks appeared on both mullions at first full cycle to 0.125 % drift for specimen BH-WOA-V. During drifts of 0.25% to 1%, large diagonal shear cracks developed and caused shear failure on both mullions for all specimens. At 0.5% drift, a lot of fine flexural cracks developed into inclined shear cracks on columns and conversely, small flexural cracks existed on the beams at 2% drift.

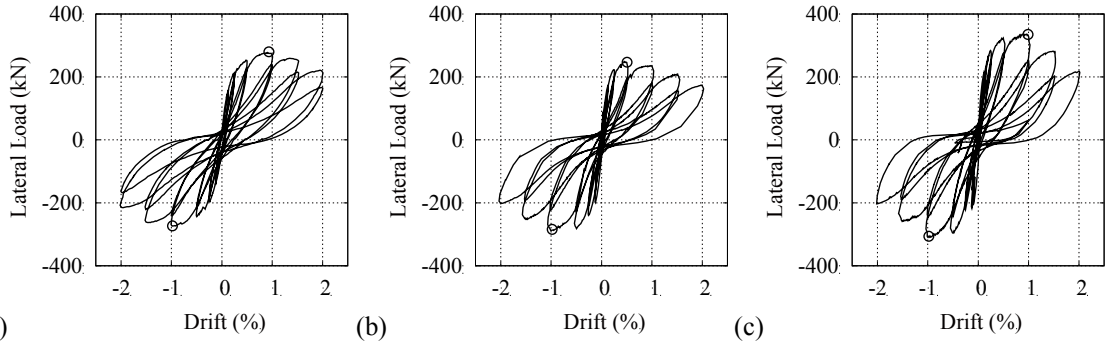

Figure 4. Lateral load-drift relationships: (a) B-WOA, (b) BH-WOA-V, (c) BH-WOA-VH

Table 4. Ultimate lateral load and shear stress

Specimen	B-WOA	BH-WOA-V	BH-WOA-VH
Ultimate lateral load (kN)	277	289	336
Ultimate drift (%)	1.0	0.5	1.0
Average shear stress at ultimate drift, τ_u (MPa)	2.50	2.62	3.04
Normalized shear stress, τ_u / f'_c	0.12	0.11	0.12

Figure 5. Crack patterns at first full cycle to 1% drift: (a) B-WOA; (b) BH-WOA-V, and (c) BH-WOA-VH

3.2 Vertical move displacement of points

To investigate interaction of deformation between mullions and beams, vertical move displacement of characteristic points on the specimens BH-WOA-V and BH-WOA-VH, as shown in Figure 6(a), were measured by LVDTs. The LVDTs installed on mullions are displaced of 20 mm from the end of mullion and opening. The measured points (A to D) are classified into two parts: left and right part. Figure 6(b) and (c) show relationship between vertical move displacement at each point and lateral drift for left and right part, respectively, at drift in positive direction. The vertical axis represents the vertical move displacement and the horizontal axis represents story drift. The positive and negative values means upward and downward movement, respectively. All move displacements for both specimens on the right part decrease with a decrease of drift, whereas the move displacement except point D for specimen BH-WOA-VH increases with a decrease of drift on the left part. The mullion on the left side for specimen BH-WOA-VH moves upward by deformation. The amount of move displacements for specimen BH-WOA-VH are smaller than that of specimen BH-WOA-V on both parts, which represents that deformation of mullions are different between both specimens.

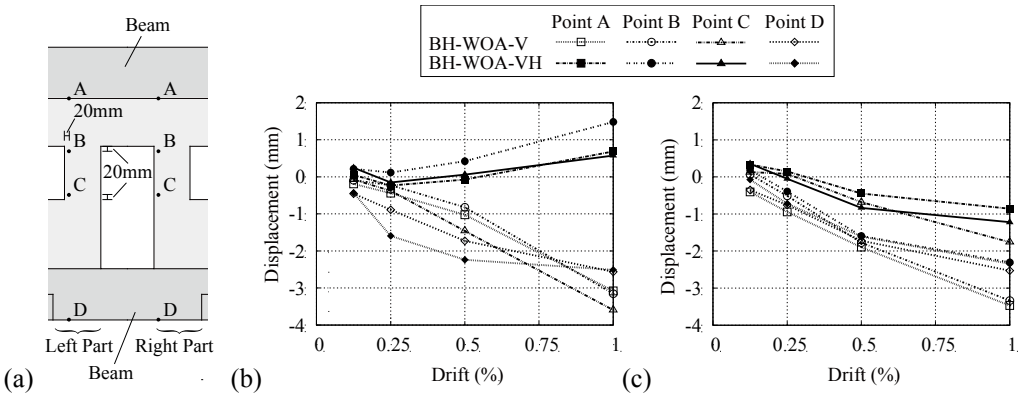

Figure 6. Vertical move displacement: (a) positions of measured point; (b) left part; and (b) right part

3.3 Deformation diagram

Deformation diagram of mullions for specimen BH-WOA-V and BH-WOA-VH at each drift in positive direction illustrated in Figure 7. The horizontal axis and vertical axis represent horizontal deformation and vertical deformation, respectively. The diagram are drawn with an assumption that the point at bottom left corner is fixed. Note that the load is applied from left to right, and the deformations are magnified by five times. Figure 7 shows that the estimated diagram of the left mullion rotates with increase of drift for both specimens, which represents that flexural deformation is dominant on the left mullion. On the other hand, shear deformation are dominant in the right mullion. These deformations are assumed to be given by deformation of frame: at drift in positive direction, the left mullion is subject to tension due to flexural bending of frame and both mullions are forced to deform by deflection of beam.

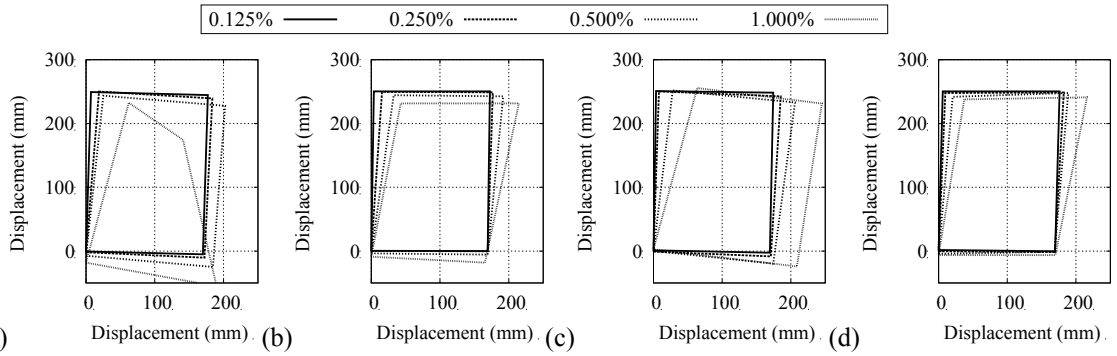

Figure 7. Deformation diagram: (a) and (b) are mullion on the left and right side, respectively, for specimen BH-WOA-V; (c) and (d) are mullion on the left side and right side, respectively, for specimen BH-WOA-VH

3.4 Failure mechanism

Both mullions were failed in shear at 1% drift; however, sequence of crack patterns are different between the left and right mullions. Flexural cracks appeared prior to shear cracks on the left mullion for all the specimens whereas shear cracks appeared only on the right mullion, and thereby the shear failure occurred on the right mullion earlier than that on the left one. To prevent premature shear failure of mullions, this failure mechanism should be investigated. As previously discussed, based on the observation that failure mechanism of mullions is assumed to be

associated with beam deformation, effect of axial force of mullion are evaluated using experimental results.

The axial force N are obtained by equilibriums of forces by reinforcement and concrete acting in plane with cross section of mullion. The axial force of reinforcement were calculated by stain given by average curvature assumed by LVDTs' displacement. Simultaneously compression force by concrete were assumed by triangular stress distribution. If the stress reaches compressive strength, stress block method (American Concrete Institute, 2008) are applied. The axial forces N at each drift in positive direction for specimens BH-WOA-V and BH-WOA-VH are shown in Table 4. The plus and minus sign in axial force represent compression and tension, respectively. The flexural strength V_b and shear strength V_s (Japan Building Disaster Prevention Association, 2005) are derived by followings. Note that there is no boundary column in mullion, then first term in numerator of the right side of Equation 2 is neglected.

$$V_b = \frac{a_t \cdot \sigma_{sy} \cdot l_w + 0.5\sum\left(a_{wv} \cdot \sigma_{wy}\right) \cdot l_w + 0.5Nl_w}{h_w/2} \tag{2}$$

$$V_s = \left(\frac{f'_c}{20} + 0.5p_w \cdot \sigma_{wy}\right) \cdot t_w \cdot l_{w0} \tag{3}$$

where a_t is area of longitudinal reinforcement in boundary column (=0), σ_{sy} is yield strength of longitudinal reinforcement in boundary column, l_w is effective depth of mullion (=0.8l_{w0}), l_{w0} is depth of mullion, a_{wv} is vertical reinforcement of mullion, σ_{wy} is yield strength of vertical reinforcement of mullion, N is axial force, h_w is height of mullion, f'_c is concrete compressive strength, p_w is ratio of horizontal reinforcement, and t_w is thickness of mullion.

The failure mechanism can be assumed by a ratio of V_s/V_b, which is an index to classify failure mechanism. If the V_s/V_b index is less than one, then shear failure is assumed. The shear strength V_s is constant at all drifts; however, the flexural strength V_b shows trend of increase with an increase of drifts in accordance with axial force N for both specimens. For the left mullion of specimen BH-WOA-V at drifts of 0.125% to 0.5%, flexural yielding before shear failure is assumed, but at subsequent drift of 0.25%, shear failure is assumed. This transition of failure mechanism is agreed with observed damage. On the other hand, for the right mullion of both specimens, the failure mechanism is assumed as shear failure at all drifts because large axial force is assumed. The failure mechanism at failure drift for both left and right mullions of specimen B-WOA-V are agreed with experimental results; however, for the left mullion of specimen BH-WOA-VH at 1% drift, failure mode of flexural yielding is not agreed with experimental results because tension displacements were observed on the left mullion at all drifts.

The shear force V_a on mullion at failure drift can be assumed by a gross area of mullion times average shear stress shown in Table 3, and the failure mechanism are confirmed by comparing the shear force V_a with shear strength V_s. For specimen BH-WOA-V the shear force V_a of 18kN is almost agreed with shear strength V_s at 1.0% drift; however, the shear force V_a of 21kN at 1.0% drift for specimen BH-WOA-VH is not agreed with the shear strength V_s of both left and right mullions. Because the horizontal reinforcement have not reached yield strain for specimen BH-WOA-VH, the shear strength is not archived. The shear strength V_s assumed by measured maximum stress of vertical reinforcement in mullion comes to be 25kN and is almost agreed with prediction. Thus, to prevent premature shear failure of mullion, it is important to design axial force as well as increasing reinforcement because increase of axial force involves with deformations lead to fail in shear.

Table 5. Axial force and failure mechanism at each drift in positive direction

		Drift (%)	N (kN)	V_s (kN)	V_b (kN)	V_s/V_b	Failure mode
BH-WOA-V	Left	0.125	13.7	17.7	15.5	1.14	Flexural yielding
		0.25	14.6	17.7	15.9	1.11	Flexural yielding
		0.5	-14.6	17.7	7.99	2.22	Flexural yielding
		1.0	95.7	17.7	60.1	0.29	Shear failure
	Right	0.125	12.5	17.7	14.8	1.20	Flexural yielding
		0.25	121.2	17.7	73.9	0.24	Shear failure
		0.5	124.3	17.7	75.6	0.23	Shear failure
		1.0	100.8	17.7	62.8	0.28	Shear failure
BH-WOA-VH	Left	0.125	-1.98	45.5 (24.8)	21.3	2.14	Flexural yielding
		0.25	-17.3	45.4 (24.8)	21.3	2.13	Flexural yielding
		0.5	-20.0	45.4 (24.8)	21.3	2.13	Flexural yielding
		1.0	-14.1	45.4 (24.8)	21.3	2.13	Flexural yielding
	Right	0.125	48.4	45.5 (24.8)	47.6	0.96	Shear failure
		0.25	93.9	45.4 (24.8)	72.4	0.62	Shear failure
		0.5	145.0	45.4 (24.8)	100.2	0.45	Shear failure
		1.0	149.7	45.4 (24.8)	102.7	0.44	Shear failure

4 CONCLUSIONS

The main purpose of this research was to investigate behavior of mullions formed in non-structural RC walls based on the experimental program carried out on one-bay frame with mullions formed in non-structural wall. The main findings can be summarized as follows: 1) flexural behavior and shear behavior dominate in mullions in accordance with flexural bending behavior of wall; and 2) axial force of mullions increase correspond to increase of drift which might lead to shear failure even if sufficient shear reinforcement are arranged, and failure mechanism assumed considering variable axial force is agreed with experimental results.

ACHKNOWLEDGEMENT

This work was supported by JSPS KAKENHI Grant Number 24686063. The authors wish to acknowledgement the supplier of the reinforcement; JFE Techno-wire Co., Ltd.

REFERENCES

American Concrete Institute. 2008. *Building Code Requirements for Structural Concrete (ACI 318-08) and Commentary*. Michigan: American Concrete Institute.

Japan Building Disaster Prevention Association. 2005. *Seismic Evaluation and Retrofit*. Tokyo: Japan Building Disaster Prevention Association.

Okubo, K., Shiohara, H., Darama, H. and Tamura, K.. 2009. Non-Structural Reinforced Concrete Partition Walls as Secondary Damping Devices, San Francisco, *Proceedings of ATC and SEI Conference on Improving the Seismic Performance of Existing Buildings and Other Structures*, 1034-1045.